

Article

# Kinetics of Nanostructuring Processes of Material Surface under Influence of Laser Radiation

Alexei Khomenko <sup>1,2,\*</sup> , Olga Yushchenko <sup>1</sup> and Anna Badalian <sup>1</sup>

<sup>1</sup> Department of Applied Mathematics and Complex Systems Modeling, Sumy State University, 40007 Sumy, Ukraine; o.yushchenko@phe.sumdu.edu.ua (O.Y.); a.badalyan@mss.sumdu.edu.ua (A.B.)

<sup>2</sup> Peter Grünberg Institut-1, Forschungszentrum-Jülich, D-52425 Jülich, Germany

\* Correspondence: o.khomenko@mss.sumdu.edu.ua; Tel.: +38-(0542)-33-3155

Received: 12 October 2020; Accepted: 17 November 2020; Published: 20 November 2020



**Abstract:** In this paper, further research is conducted for a synergetic model that describes the state of the material surface in the process of laser irradiation. Namely, the previously studied approach of mutually coordinated behavior of the relaxation field, concentration of relaxation zones, and field of stress is supplemented with a nonlinear term. It is shown that, using this model, we can describe the behavior of different types of systems. During the analysis, five stationary states were found which correspond to different modes of formation of relaxation areas on the surface. The regions of parameters are found at which one or another mode of the system behavior is established. Phase portraits are constructed for each mode and the kinetics of the system is described. The obtained results qualitatively coincide with the experimental data.

**Keywords:** nanostructure; relaxation zone; self-organization; Lorenz system; phase diagram; phase portrait

**MSC:** 82-02; 82B26; 82C26; 37F99

## 1. Introduction

Various methods for obtaining nanoscale structural objects on the surface of solids are of great interest for mechanics, metallurgy, chemistry, and solid state physics. Often such structures are generated during laser irradiation of the material, they are usually localized in the surface layer of solids, but mainly affect the various properties of the material [1]. Such nanocoatings are widely used in different fields of technology and science for a variety of tasks [2]. In electronics, electrical engineering, spectroscopy, and optics, such tasks are reduced to the improvement of thermal, absorbing, radiating, and electric properties of materials. For example, [3] discusses centimeter-sized chemical vapor deposition synthesis with a laser of a free-standing, continuous and stable single-layer amorphous carbon, topologically different from disordered graphene. In the chemical industry, they boil down to the initiation of catalytic capabilities of the material or to the change of surface wetting properties. The increasing of the wear resistance by applying nanocoating on the walls of metals and ceramics, that work in conditions of severe corrosion, improves the performance of various devices and reduces friction between individual parts. Thus, the development of new approaches to the physical foundations of structuring, which lead to the formation of nanoscale reliefs on the surface of superhard ceramic materials, diamond films, metals and alloys, polymers, and biomaterials, becomes relevant.

Typically, for nanostructuring by laser radiation, one can use the interference effect of two or more laser beams or templates projected onto a surface. The result is a spatial modulation of the distribution of the incident radiation intensity with characteristic nanoperiods [1]. Unlike methods where electron or ion beams are used for the process of material nanostructuring, laser processing methods do not require placing the beam and the irradiated sample in a special vacuum chamber. Therefore, we will consider further the creation of surface nanostructures with a simpler method, i.e., using a laser beam.

The structural states obtained after laser treatment are very diverse, but for any region, its shape changes after the transformation of the old phase of the region into a new one. As a result, a characteristic relief appears on the flat surface of the sample with individual parameters of macroscopic strain for each type of transformation. The method of creating nanostructured objects on the surface of material by a single laser beam is called the method of direct laser nanostructuring. Compared to other methods, it is more flexible and easy to implement. When using a single laser beam of a small size, the high locality of action is achieved; it is fixed by the size of one beam and the step of its scanning on the surface. The process of scanning the surface using radiation with a high frequency of repetitive pulses makes it possible to process large surfaces with a sufficiently high value of spatial resolution.

As the experimental data show, the method of direct laser nanostructuring consists of multiple exposures to one laser beam on the sample under study. Irradiation of the material can be carried out both with a stationary laser beam and with its movement along the surface at a given speed. To simulate the processes of nanostructuring of matter under the action of short laser pulses on the surface of a solid, it is necessary to understand the arising physical processes [1–8]. Since these processes take place in extremely small volumes and time intervals, high heating and cooling rates appear, as well as large spatial temperature gradients. This leads to various phase transitions (melting, evaporation), thermionic emission, gas desorption, thermomechanical effects (thermal expansion, thermal stress), and structural changes [1,5–8]. Understanding which of these processes is predominant, it is possible to develop a model for estimating the characteristic parameters of the resulting nanostructures.

Many processes (for example, melting of a material by continuous laser radiation) are well described theoretically. It was found experimentally for the melting regime that the involved mechanism is thermal. For example, in [8], nanostructures are presented in the form of bulges with rounded tops on the germanium surface. These structures were obtained by irradiating the sample with an ArF laser at a total energy density in the center of the spot of about  $4 \text{ J/cm}^2$ , the number of pulses is 20, and a repetition rate of 2 Hz. The period of the structures is from 40 to 120 nm, their amplitude is 40–70 nm. The rounded shape of the obtained nanoreliefs indicates the surface melting by laser radiation and further crystallization. As a result, the final structure of the material surface, on the one hand, is determined by the dynamics of the melt movement, and on the other, by the kinetics of the crystallization process. Moreover, a theoretical description of the kinetics of such processes is insufficient. The most general theoretical approach is based on the analysis of the distribution function of the number of particles of the crystalline phase.

For other examples, the characteristic formation of cracks or protruding points on the surface indicates deformation of the material due to phase and structural transformations. A similar experiment is described in [4,7,8], where an ArF laser with a laser energy density of  $0.18 \text{ J/cm}^2$  was used. As a result, cracking of the surface layer and features of the relief in the form of protruding points with sizes from 1 to  $5 \mu\text{m}$  were found. Since, in this case, under the influence of laser radiation material has a high thermal stress, the deforming process under these conditions is accompanied by residual strain. The appearance of the residual deformation is due to inelastic effects and rearrangement of crystal defect structure. In this case, the mechanism of absorption of laser radiation by a metal surface during the formation of surface nanostructures is nonlinear and has a heterogeneous character [4,6,7].

Recently, studies [4,7,9] give gradual progress in describing the basics and patterns of formation of real surface structures. The current state of this research requires: firstly, the accumulation of much more practical experience in studying the mechanisms and processes of the nanostructures formation; secondly, the creation of new theories that help to explain the operation of such mechanisms [2,10–17].

Along this line, the governing evolution equations of the Lorenz-type for relaxation and stress fields, as well as concentration of relaxation zones are determined in Section 2. The model permits to describe the nanostructuring processes of material surface under influence of laser radiation. In contrast to the previous approaches, here nonlinear effects in the mechanism of nanostructure formation are considered using a nonlinear relationship between the relaxation and stress fields with the rate of change of the relaxation field. Section 3 represents steady-state analysis of the basic relations in terms

of effective energy that allows us to depict the formation of stationary nanostructures. The description of the resulting nanostructured objects is carried out using the adiabatic approximation taking into account that evolution of stresses and concentration of relaxation zones follow changes of relaxation field. The diagram is built determining residual stress established due to relaxation, ratios of relaxation times of basic parameters and coupling constants, and specifying the types of the stationary modes. In Section 4, the expressions for Lyapunov exponents are obtained, which define the stability of steady states and the phase dynamics of nanostructuring processes. Using the three-dimensional phase portraits, formation mechanisms of different nanostructures are described. Section 5 is devoted to brief conclusions.

## 2. Phenomenological Model

At a sufficiently high stress, the process of deformation of a solid is accompanied by residual strain, the appearance of which relates to the rearrangement of the defective crystal structure and with inelastic effects. Stress relaxation can be localized through the formation of the relaxation zones and zones of a new structure [4]. These processes are associated with the collective behavior of the excited interacting atoms, making the relaxation process nonlinear.

Exposing a solid to the high mechanical stresses caused by a laser beam can excite many atoms. In an excited state, an atom travels a lattice parameter distance during the Debye time. As a result, the position of the atom, averaged over a macroscopically small time, cannot be associated to a particular site. Then, due to nucleation of new structure and relaxation zones, the relaxation of this excited state can occur. Depending on the external conditions and the stage of the deformation process development, the relaxation zones can be assigned to: groups of dislocations or disclinations; groups of atoms, forming the clusters; groups of vacancies, forming the dislocation loops; micropores; microcracks, etc.

Thus for a deformable solid the thermodynamic potential can be written [1,4] as

$$d\Phi = -SdT + \sum_k^{N_1} A_k da_k + \sum_k^{N_2} x_k d\zeta_k, \quad (1)$$

where  $S$  is the entropy that characterizes the unbalanced (disordered) state of the system,  $a_k$  are the external parameters determining the solid state;  $A_k$  are the general forces associated with the external parameters  $a_k$ ;  $\zeta_k$  are the internal parameters characterizing the solid state with given temperature  $T$  and external parameters  $a_k$ ; parameters  $x_k$  determine the internal field;  $N_1$  and  $N_2$  are the corresponding number of external and internal parameters, respectively.

The disordered state of an elastically deformed solid is characterized by the strain tensor  $\varepsilon_{ik}$ , the stress tensor  $\sigma_{ik}$ , the temperature  $T$ , and additional internal parameters of the state  $\psi_{ik}^{(1)}$ ,  $\psi_{ik}^{(2)}$ , ...,  $\psi_{ik}^{(N)}$ , which determine the deviation degree of the system state from the order for given  $T$  and  $\varepsilon_{ik}$ . The number of internal state parameters  $\psi_{ik}^{(\eta)}$  together with  $T$  and  $\varepsilon_{ik}$  can completely determine the system state. Using the equation [1] where the process rate depends linearly on the thermodynamic force, one can determine the rate of change for the relaxation tensor  $\dot{\psi}_{ik}^{(\eta)}$ :

$$\frac{\partial \Phi}{\partial \psi_{ik}^{(\eta)}} = \sum_{\theta} h_{iklm}^{(\eta,\theta)} \dot{\psi}_{lm}^{(\theta)}, \quad (2)$$

where  $\Phi$  is the density of the thermodynamic potential for the deformable solids;  $h_{iklm}^{(\eta,\theta)}$  are the material constants. In such equation the stationary states, corresponding to different spatial forms, are stable [1]. Analyzing the deformed solid behavior, the set of relaxation parameters  $\psi_{ik}^{(\eta)}$  is presented as one parameter through the residual strain  $\varepsilon_{ij}^0(\mathbf{r}, t)$ . So, the field of the relaxation process is determined by the mesoscopic relaxation parameter:

$$\varphi_{ik}(\mathbf{r}, t) = \frac{1}{V_0} \int_{V_0} \varepsilon_{ij}^0(\mathbf{r}, t) dV, \quad (3)$$

where  $V_0$  is the volume, on which the averaging is performed.

Thus, the structural state transitions for a solid surface under laser treatment can be represented by the self-consistent behavior of the parameters: the field of the relaxation process, which is specified by the parameter  $\varphi_{ik}(\mathbf{r}, t)$ , field of stress (or external load)  $\sigma_{ik}(\mathbf{r}, t)$ , and the concentration of relaxation zones  $n(\mathbf{r}, t)$ . The resulting time dependencies for  $\varphi_{ik}(\mathbf{r}, t)$ ,  $n(\mathbf{r}, t)$ ,  $\sigma_{ik}(\mathbf{r}, t)$  correspond to the system of three nonlinear differential equations

$$\frac{\partial \varphi_{ik}}{\partial t} = -\frac{\varphi_{ik}}{\tau_\varphi} + a_\varphi n - a_{\varphi\sigma} \varphi_{ik} \sigma_{ik}^2, \quad (4)$$

$$\frac{\partial n}{\partial t} = -\frac{n}{\tau_n} + a_n \varphi_{ik} \sigma_{ik}, \quad (5)$$

$$\frac{\partial \sigma_{ik}}{\partial t} = \frac{\sigma_0 - \sigma_{ik}}{\tau_\sigma} - a_\sigma \varphi_{ik} n. \quad (6)$$

Similarly to the Lorenz system [18–26] in the Equations (4)–(6), the relaxation field  $\varphi_{ik}(r, t)$  acts as order parameter. For the disordered state  $\varphi_{ik} = 0$ , that is, there is no relaxation field. The concentration of relaxation zones  $n$  is a field conjugated to order parameter. In this case the role of third (control) parameter is played by the stress field  $\sigma_{ik}(r, t)$ . The relaxation times for the specified parameters correspond to  $\tau_\varphi, \tau_n, \tau_\sigma$ ;  $a_\varphi, a_{\varphi\sigma}, a_n, a_\sigma$  are the positive coupling constants. The applied external load is determined by value  $\sigma_0 = const$  and corresponds to the residual stress that is established due to relaxation process.

The first terms in the right-hand sides of the Equations (4)–(6) describe, respectively, the process of relaxation damping, the relaxation zones collapse and stress relaxation in the linear approximation, when the mutual influence of the parameters is not taken into account. The second and third terms illustrate linear and nonlinear relations during the relaxation. For the first equation, for example, this relates to the relaxation field generation because of relaxation zones formation and reverse nonlinear influence of stress field. In the second one, it consider the effect of the relaxation  $\varphi_{ik}(\mathbf{r}, t)$  and stress fields  $\sigma_{ik}(\mathbf{r}, t)$  on the origin of the relaxation zones. For the third equation, it reflects the influence of the relaxation field and concentration of relaxation zones on changes of the stress field. In contrast to works [1,6,7] in our model, the Equation (4) takes into account the nonlinear relationship between the rate of change in the relaxation field (associated with residual strain) and the stress field.

Because of large number of constants in the system (4)–(6), it is convenient to use dimensionless quantities for basic parameters: time, relaxation field (order parameter), concentration of relaxation zones (conjugate field) and stress (control parameter). We used parameters of the original system to define the scales. For time it is possible to use the following scale

$$t_s = \tau_\varphi. \quad (7)$$

For the control parameter (field of stress) we have the scale

$$\sigma_s = (\tau_\varphi a_\varphi \tau_n a_n)^{-1}. \quad (8)$$

For the order parameter (field of relaxation) we select the following scale

$$\varphi_s = (a_\sigma \tau_\sigma a_n \tau_n)^{-1/2}. \quad (9)$$

Scale for the conjugate field (concentration of relaxation zones) is determined by

$$n_s = (a_\varphi \tau_\varphi \sqrt{a_\sigma \tau_\sigma \tau_n a_n})^{-1}. \quad (10)$$

Hereinafter, as the basic parameters of the system (relaxation field, concentration of relaxation zones and stress) we have in mind their dimensionless analogues. As a result, the dimensionless synergetic system of three equations allows to present in a self-consistent way the transition between different solid surface states under the laser radiation treatment. It reads as follows

$$\frac{d\varphi_{ik}}{dt} = -\varphi_{ik} + n - \alpha\varphi_{ik}\sigma_{ik}^2, \quad (11)$$

$$\delta\frac{dn}{dt} = -n + \varphi_{ik}\sigma_{ik}, \quad (12)$$

$$\gamma\frac{d\sigma_{ik}}{dt} = \sigma_0 - \sigma_{ik} - \varphi_{ik}n, \quad (13)$$

where we have introduced the relations between the relaxation times of main parameters

$$\delta = \frac{\tau_n}{\tau_\varphi}, \quad \gamma = \frac{\tau_\sigma}{\tau_\varphi} \quad (14)$$

and positive constant

$$\alpha = \frac{a\varphi\sigma}{\tau_\varphi(\tau_n a_n a_\varphi)^2}. \quad (15)$$

### 3. Steady State Analysis

It is known from the experiment that order parameter (relaxation parameter  $\varphi_{ik}$ ) usually has the greatest relaxation time. Thus field conjugated to order parameter (or concentration of relaxation zones  $n$ ) and the control parameter (field of stress  $\sigma_{ik}$ ) follow the changing of the order parameter  $\varphi_{ik}$ . As a result, we get the so-called adiabatic approximation

$$\tau_\varphi \gg \tau_n, \tau_\sigma \quad (16)$$

or

$$\delta, \gamma \ll 1. \quad (17)$$

Using approximation (17) we can neglect the time derivatives in the left-hand sides of the second and third equations of system (11)–(13). As a result, we get dependence of the stationary stress on the relaxation field

$$\sigma_{ik} = \frac{\sigma_0}{1 + \varphi_{ik}^2}. \quad (18)$$

For different values of the external load the corresponding dependence is shown in Figure 1a.

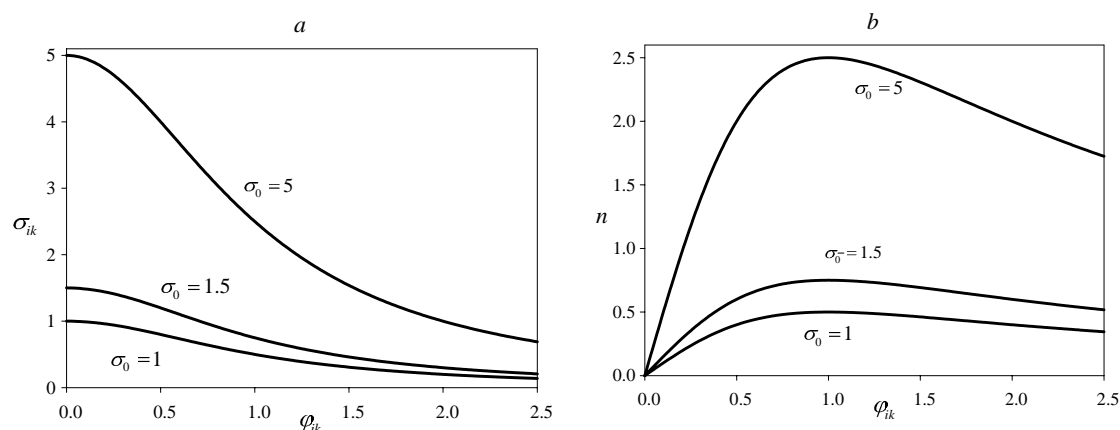


**Figure 1.** Dependence of the loads field (a) and concentration of relaxation areas (b) on the relaxation field for various values of  $\sigma_0$ .

For the relaxation zones concentration we get the stationary dependence

$$n = \frac{\sigma_0 \varphi_{ik}}{1 + \varphi_{ik}^2}. \quad (19)$$

Similar dependence of concentration of relaxation zones for different values of external load is shown in Figure 1b. Figure 1 shows that increase in the value of the relaxation parameter in the interval limited by the maximum value  $\varphi_s$  leads to increase in the concentration of relaxation areas and the decrease in the value of the stress field below the level  $\sigma_0$  defined by the applied external stress.

Inserting Equation (19) into the first formula of the basic system (11) we obtain

$$\frac{d\varphi_{ik}}{dt} = -\varphi_{ik} - \alpha \varphi_{ik} \sigma_{ik}^2 + \frac{\sigma_0 \varphi_{ik}}{1 + \varphi_{ik}^2}. \quad (20)$$

Thus, we arrive to the resulting differential equation in the Landau-Khalatnikov form

$$\frac{d\varphi_{ik}}{dt} = -\frac{\partial E}{\partial \varphi_{ik}}, \quad (21)$$

where  $E$  is the effective energy which characterizes the system state. The minimum of this energy corresponds to the stationary state of the system. Then, at zero value of the parameter  $\varphi_{ik}$  the minimum is realized. It is responsible to the absence of the relaxation zones on the surface. In the final form, we get an effective energy

$$E = \frac{1}{2} \left\{ \varphi_{ik}^2 - \frac{\alpha \sigma_0^2}{1 + \varphi_{ik}^2} - \sigma_0 \ln(1 + \varphi_{ik}^2) \right\}. \quad (22)$$

Analyzing the minima for the effective energy at non-zero values of the parameter  $\varphi_{ik}$ , we find the stationary values of the relaxation parameter. They correspond to the states of the relaxation zones formation on the solid surface under the treatment of laser radiation

$$\begin{aligned} \varphi_{ik}|_1 &= 0, \\ \varphi_{ik}|_{2,4} &= \pm \sqrt{\frac{\sigma_0}{2} \left[ 1 + \sqrt{1 - 4\alpha} \right] - 1}, \\ \varphi_{ik}|_{3,5} &= \pm \sqrt{\frac{\sigma_0}{2} \left[ 1 - \sqrt{1 - 4\alpha} \right] - 1}. \end{aligned} \quad (23)$$

The corresponding stationary values of the concentration of relaxation areas and loads are calculated by substituting (23) into the Equations (18) and (19).

As can be seen from the Equations (23), the last four states are realized only when the parameter  $\alpha$  is less than the value  $1/4$ . The condition for the existence of points  $\varphi_{ik}|_{2,4}$  is written as

$$\sigma_0 > \frac{2}{1 + \sqrt{1 - 4\alpha}}. \quad (24)$$

Moreover, points  $\varphi_{ik}|_{3,5}$  are realized only in the region

$$\sigma_0 > \frac{2}{1 - \sqrt{1 - 4\alpha}}. \quad (25)$$

The phase diagram, indicating the regions of the existence of energy minima (23), is shown in Figure 2. Region  $a$  in the phase diagram corresponds to the existence of only one minimum  $\varphi_{ik}|_1$ . In region  $b$  more minima  $\varphi_{ik}|_{2,4}$  appear, but in region  $c$  all possible solutions (23) are realized. The corresponding points on the phase diagram denote the sets of parameters  $\alpha, \sigma_0$  for which the energy of the system was plotted for each of the regions (see Figure 3).

For region *a* (see Figure 3a) this energy has only zero minimum and monotonically increasing form. This is the case of absence of the relaxation zones. For region *b*, the nonzero minima are realized (see Figure 3b). Thus, there are solutions  $\varphi_{ik|2A}$ , which correspond to the formation of relaxation areas on the surface of the material irradiated with laser light. In this case, the zero solution becomes unstable (maximum on the corresponding dependence). Figure 3c (intermediate state) characterizes the coexisting of two stable states. This means that relaxation zones are formed discontinuously by analogy with a first-order phase transition.

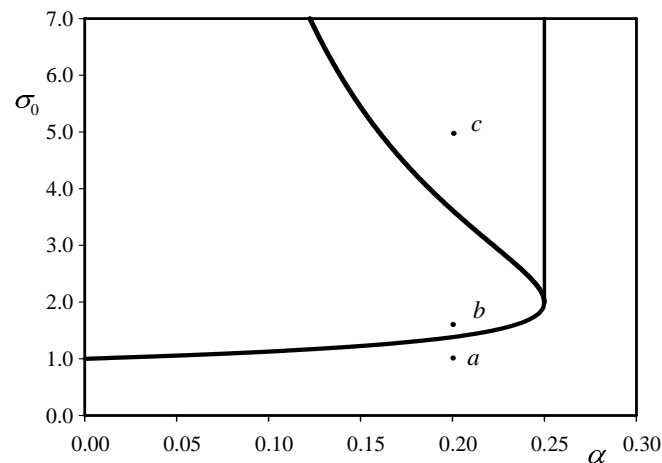


Figure 2. Phase diagram of the system.

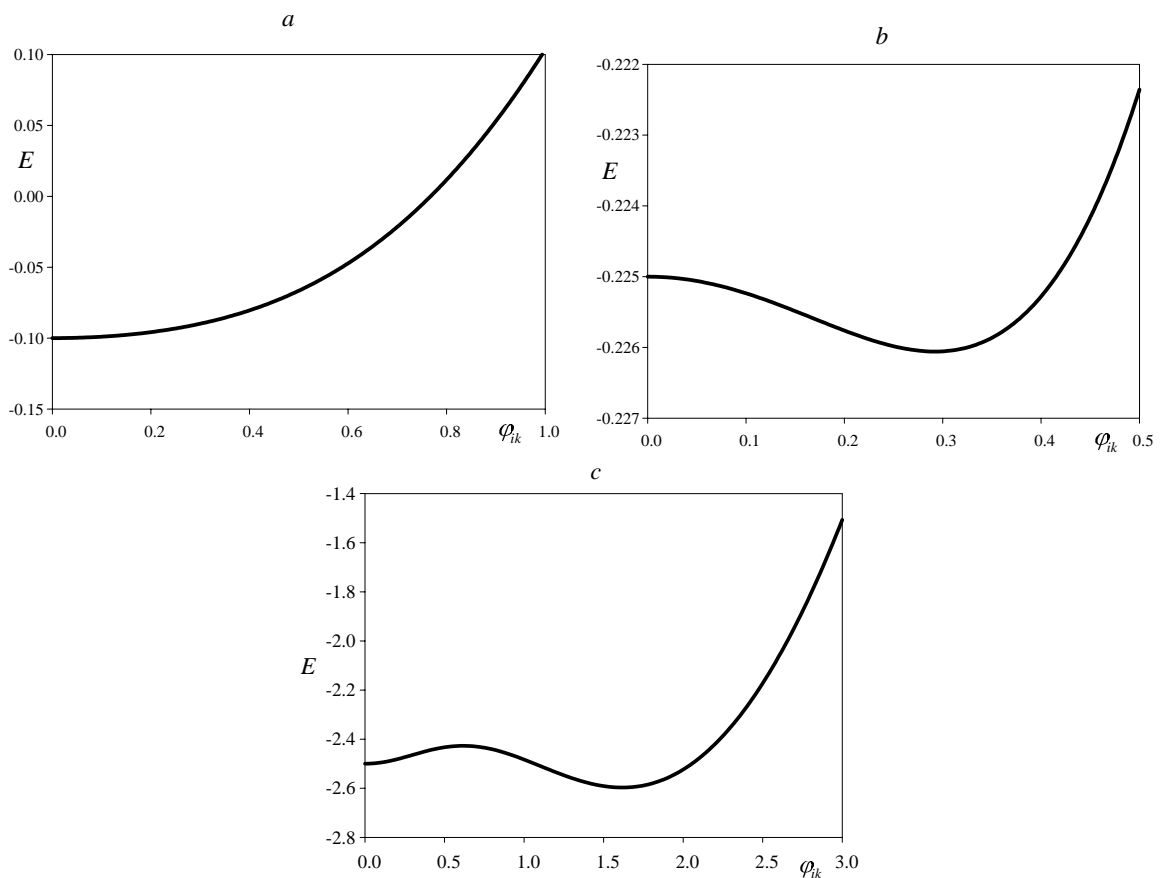


Figure 3. Effective system energy. (a–c) are constructed for the parameters indicated by points in the phase diagram (see Figure 2).

#### 4. Phase Portraits

We will seek a solution of the system of differential equations near a stationary state in the form [26,27]

$$\varphi_{ik} = \varphi_0 + ae^{\lambda t}, \quad (26)$$

$$n = n_0 + be^{\lambda t}, \quad (27)$$

$$\sigma_{ik} = \sigma_{00} + ce^{\lambda t}, \quad (28)$$

where  $\lambda$  is an unknown Lyapunov exponent,  $\varphi_0, n_0, \sigma_{00}$  are the stationary state values for the relaxation parameter, concentration, and stress, respectively. The amplitudes  $a, b$  and  $c$  correspond to the small deviations from the stationary state. Inserting (26)–(28) into (11)–(13) we get the system of equations

$$a\lambda e^{\lambda t} = -\varphi_0 - ae^{\lambda t} - \alpha\varphi_0\sigma_{00}^2 - \alpha\sigma_{00}^2ae^{\lambda t} - 2\alpha\varphi_0\sigma_{00}ce^{\lambda t} + n_0 + be^{\lambda t}, \quad (29)$$

$$\delta b\lambda e^{\lambda t} = -n_0 - be^{\lambda t} + \varphi_0\sigma_{00} + a\sigma_{00}e^{\lambda t} + \varphi_0ce^{\lambda t}, \quad (30)$$

$$\gamma c\lambda e^{\lambda t} = \sigma_0 - \sigma_{00} - ce^{\lambda t} - \varphi_0n_0 - n_0ae^{\lambda t} - \varphi_0be^{\lambda t}, \quad (31)$$

which are obtained for the first order for  $a, b$ , and  $c \ll 1$  (for zero-order  $a, b, c \ll 1$  equations give stationary values).

Let us analyze the first stationary state

$$\varphi_0 = n_0 = 0, \quad \sigma_{00} = \sigma_0, \quad (32)$$

which corresponds to the absence of the formation of relaxation areas on the surface of the material after laser treatment. Then, the system (29)–(31) takes the form

$$0 = (\lambda + 1 + \alpha\sigma_0^2)a - b, \quad (33)$$

$$0 = -\sigma_0a + (\delta\lambda + 1)b, \quad (34)$$

$$0 = (\gamma\lambda + 1)c. \quad (35)$$

The condition for solving the system (33)–(35) is the equality to zero of its determinant:

$$(\gamma\lambda + 1) \left[ (\lambda + 1 + \alpha\sigma_0^2) (\delta\lambda + 1) - \sigma_0 \right] = 0. \quad (36)$$

The three roots of the Equation (36) have the form

$$\begin{aligned} \lambda_1 &= -1/\gamma, \\ \lambda_{2,3} &= \frac{1}{2\delta} \left\{ -(1 + \delta + \alpha\delta\sigma_0^2) \pm \sqrt{(1 + \delta + \alpha\delta\sigma_0^2)^2 - 4\delta(1 - \sigma_0 + \alpha\sigma_0^2)} \right\}. \end{aligned} \quad (37)$$

Moreover, the first root  $\lambda_1$  is always negative. The remaining two complex-conjugate roots also have a negative real part. The type of stability of a stationary point depends on the type of roots.

In the case of formation of relaxation zones on the surface of the material, the stationary values  $\varphi_{ik}|_{2,3,4,5}$  from (23) are realized. If these values are substituted into the system (29)–(31), and the corresponding determinant is equated to zero, then we obtain the cubic equation

$$\lambda^3 + A\lambda^2 + B\lambda + C = 0, \quad (38)$$

where the factors are given by the ratios



$$\begin{aligned}
 A &= 1 + \frac{4\alpha}{(1 \pm \sqrt{1-4\alpha})^2} + \frac{\delta + \gamma}{\delta\gamma}, \\
 B &= \frac{1}{\delta\gamma} \left\{ \delta + \gamma + \frac{\sigma_0(1 \pm \sqrt{1-4\alpha})}{2} + \frac{4\alpha(3\delta + \gamma)}{(1 \pm \sqrt{1-4\alpha})^2} - \frac{2\gamma + 4\alpha\delta\sigma_0}{1 \pm \sqrt{1-4\alpha}} \right\}, \\
 C &= \frac{1}{\delta\gamma} \left\{ \sigma_0 + \frac{\sigma_0(1 \pm \sqrt{1-4\alpha})}{2} - \frac{4 + 6\alpha\sigma_0}{1 \pm \sqrt{1-4\alpha}} + \frac{16\alpha}{(1 \pm \sqrt{1-4\alpha})^2} \right\}.
 \end{aligned} \tag{39}$$

In this case, the discriminant of the Equation (38) is given by the standard expression

$$\Delta = -4A^3C + A^2B^2 - 4B^3 + 18ABC - 27C^2. \tag{40}$$

If  $\Delta > 0$ , the Equation (38) has three different real roots. Equality to zero of discriminant means that two of the real roots coincide. In the situation  $\Delta < 0$ , we have one real and two complex-conjugate roots. The existence of a complex part and the sign of  $\lambda_i$  determines the type of a singular point for a given set of parameters  $\sigma_0, \alpha, \delta, \gamma$ . That is, the type of stationary mode with fixed model parameters can sometimes be determined in advance by the values of  $\lambda_i$ .

Let us analyze possible modes of behavior of the system on the basis of phase portraits [25–27]. To do this, we first find the coordinates of the singular points corresponding to the extremums of the effective energy in Figure 3 (see Table 1).

The corresponding phase portraits are shown in Figure 4. As can be seen from Figure 4a, with such a set of parameters, only a disordered state is realized, i.e., no relaxation zones are formed. In this case, the type of stability of a single point  $O$  corresponds to a stable node. In Figure 4b point  $O$  turns into a saddle, but at the same time, two stable nodes  $R_{\pm}$  appear. They characterize an ordered state, i.e., processes of formation of relaxation zones on the surface of the material. Figure 4c describes a more specific regime where three points  $O, R_{\pm}$  become stable, but two saddles  $M_{\pm}$  separate them. That is, such a case is characterized by a situation of coexistence of two states (ordered and disordered). In addition, as can be seen from the figure (points  $R_{\pm}$  are stable focuses), the processes of formation of relaxation zones on the surface of the material are of an oscillatory nature.

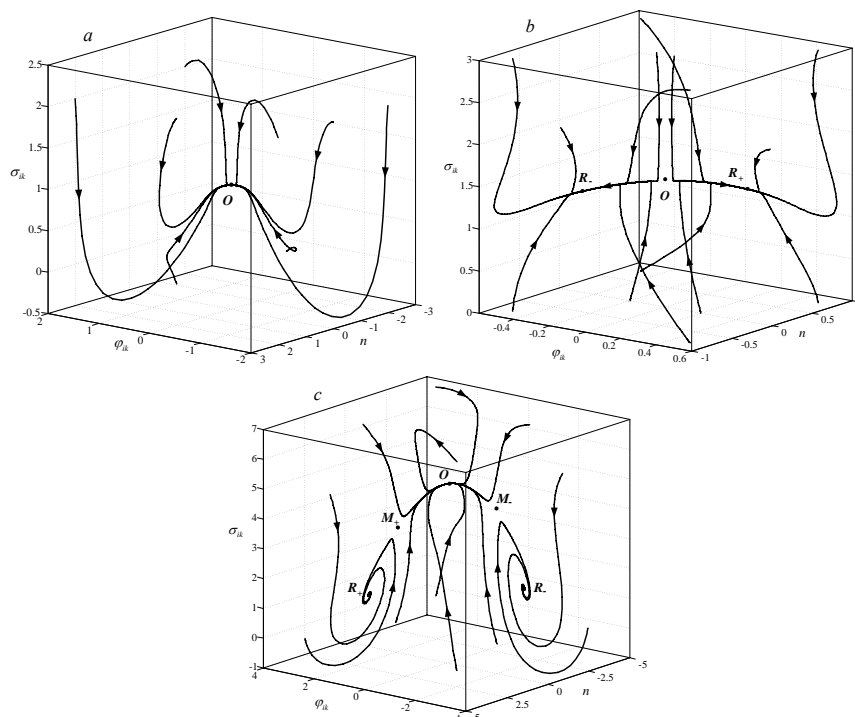


**Figure 4.** Phase portraits of the system. (a–c) are constructed for the parameters indicated by points in the phase diagram (see Figure 2).

**Table 1.** Singular points of the system for  $\delta = 1, \gamma = 1, \alpha = 0.2$ .

$\sigma_0$	Point $O$	Points $M_{\pm}$	Points $R_{\pm}$
1	0; 0; 1	–	–
1.5	0; 0; 1.5	–	$\pm 0.29; \pm 0.4; 1.38$
5	0; 0; 5	$\pm 0.62; \pm 2.24; 3.62$	$\pm 1.62; \pm 2.24; 1.28$

## 5. Conclusions

Based on the synergetic system of three differential equations, the transitions between different states of the solid surface after the nanostructuring by laser radiation were analyzed within modified theoretical model. As the order parameter, the relaxation field, which is characterized by the residual strain, was chosen. The role of the field conjugated to the order parameter is played by the concentration of the relaxation zones on the solid surface. The control parameter was found to be the stress field. As a result, the phase diagram was built, and the effective energy of the system was found. Analysis of different external loads, which correspond to the different intensities of laser radiation, has shown the existence of different regimes of phase transition. Based on phase portraits the mechanisms of transition between different conditions were considered. Indeed, the approach is general, so some broad assumptions are made about relaxation and couplings. However, in the context of the assumptions, the solutions are pointed out whose behavior depends on the intensity of laser radiation. In the long run, such dependencies may give rise to useful verification by experiment, since laser intensity is an easily adjustable experimental parameter.

**Author Contributions:** Investigation, A.K., O.Y., and A.B. All authors have read and agreed to the published version of the manuscript.

**Funding:** The work was executed under support of the Ministry of Education and Science of Ukraine within the framework of the project “Atomistic and statistical representation of formation and friction of nanodimensional systems” (No. 0118U003584).

**Conflicts of Interest:** The authors declare no conflict of interest. The funders had no role in the design of the study; in the collection, analyses, or interpretation of data; in the writing of the manuscript, or in the decision to publish the results.

## References

1. Khomich, V.Y.; Shmakov, V.A. Mechanisms of direct laser nanostructuring of materials. *Phys. Usp.* **2015**, *58*, 455–465. [[CrossRef](#)]
2. Makarov, G.N. Laser applications in nanotechnology: Nanofabrication using laser ablation and laser nanolithography. *Phys. Usp.* **2013**, *56*, 643–682. [[CrossRef](#)]
3. Toh, C.-T.; Zhang, H.; Lin, J.; Mayorov, A.S.; Wang, Y.-P.; Orofeo, C.M.; Ferry, D.B.; Andersen, H.; Kakenov, N.; Guo, Z.; et al. Synthesis and properties of free-standing monolayer amorphous carbon. *Nature* **2020**, *577*, 199–203. [[CrossRef](#)] [[PubMed](#)]
4. Khomich, V.Y.; Shmakov, V.A. Formation of periodic nanodimensional structures on the surface of solids during phase and structural transformations. *Dokl. Phys.* **2012**, *57*, 349–351. [[CrossRef](#)]
5. Apollonov, V.; Prokhorov, A.; Shmakov, A. Formation of periodic structures on the surface of solids during stress relaxation. *Sov. Tech. Phys. Lett.* **1991**, *17*, 59–63.
6. Mikolutskiy, S.I.; Tokarev, V.N.; Khomich, V.Y.; Shmakov, V.A.; Yamshchikov, V.A. Investigation of the processes of formation of nanostructures on the surface of materials under the influence of radiation from an ArF-laser. *Adv. Appl. Phys.* **2013**, *1*, 548–553.
7. Khomich, V.Y.; Shmakov, V.A. Radiation absorption by metals during the formation of surface nanostructures. *Dokl. Phys.* **2019**, *64*. [[CrossRef](#)]
8. Mikolutskiy, S.I.; Khomich, V.Y.; Yamshchikov, V.A.; Shmakov, V.A. Formation and growth of nanostructures on the surface of solids melted by laser pulses. *Nanotechnol. Russ.* **2011**, *6*, 733–738. [[CrossRef](#)]

9. Yushchenko, O.V.; Badalyan, A.Y. Theoretical model of the processes of nanostructuring the material surface under the influence of laser radiation. In Proceedings of the IEEE 8th International Conference on Nanomaterials: Applications and Properties (NAP'18), Zatoka, Ukraine, 9–14 September 2019; IEEE: New York, NY, USA, 2019; Volume 4, pp. 1–4. [[CrossRef](#)]
10. Metlov, L.S.; Myshlyayev, M.M.; Khomenko, A.V.; Lyashenko, I.A. A model of grain boundary sliding during deformation. *Tech. Phys. Lett.* **2012**, *38*, 972–974. [[CrossRef](#)]
11. Khomenko, A.; Troshchenko, D.; Metlov, L. Thermodynamics and kinetics of solids fragmentation at severe plastic deformation. *Condens. Matter Phys.* **2015**, *18*, 33004. [[CrossRef](#)]
12. Khomenko, A.V.; Prodanov, N.V.; Persson, B.N.J. Atomistic modelling of friction of Cu and Au nanoparticles adsorbed on graphene. *Condens. Matter Phys.* **2013**, *16*, 33401. [[CrossRef](#)]
13. Pogrebnjak, A.D.; Ponomarev, A.G.; Shpak, A.P.; Kunitskii, Y.A. Application of micro- and nanoprobe to the analysis of small-sized 3d materials, nanosystems, and nanoobjects. *Phys. Usp.* **2012**, *55*, 270–300. [[CrossRef](#)]
14. Goncharov, A.A.; Kononov, V.A.; Volkova, G.K.; Stupak, V.A. Size effect on the structure of nanocrystalline and cluster films of hafnium diboride. *Phys. Metal. Metallogr.* **2009**, *108*, 368. [[CrossRef](#)]
15. Prodanov, N.V.; Khomenko, A.V. Computational investigation of the temperature influence on the cleavage of a graphite surface. *Surf. Sci.* **2010**, *604*, 730–740. [[CrossRef](#)]
16. Khomenko, A.V.; Prodanov, N.V. Molecular dynamics of cleavage and flake formation during the interaction of a graphite surface with a rigid nanoasperity. *Carbon* **2010**, *48*, 1234–1243. [[CrossRef](#)]
17. Khomenko, A.V.; Prodanov, N.V. Study of friction of Ag and Ni nanoparticles: An atomistic approach. *J. Phys. Chem. C* **2010**, *114*, 19958–19965. [[CrossRef](#)]
18. Yushchenko, O.V.; Badalyan, A.Y. Statistical description of the collective motion of nanoparticles. *Phys. Rev. E* **2012**, *85*, 051127. [[CrossRef](#)]
19. Olemskoi, O.I.; Yushchenko, O.V.; Zhylenko, T.I. Study of conditions for hierarchical condensation near the phase equilibrium. *Ukr. J. Phys.* **2011**, *56*, 474–483.
20. Yushchenko, O.V.; Badalyan, A.Y. Microscopic description of nonextensive systems in the framework of the Ising model. *Ukr. J. Phys.* **2013**, *58*, 497–504. [[CrossRef](#)]
21. Olemskoi, A.I.; Yushchenko, O.V.; Badalyan, A.Y. Statistical field theory of a nonadditive system. *Theor. Math. Phys.* **2013**, *174*, 386–405. [[CrossRef](#)]
22. Yushchenko, O.V.; Badalyan, A.Y. Magnetic first-order phase transitions in nano-cluster systems within the framework of Landau approximation. *J. Nano-Electron. Phys.* **2017**, *9*, 04022. [[CrossRef](#)]
23. Yushchenko, O.V.; Rudenko, M.A. Description of the transition between different modes of nanoparticles's motion within the four-parameter Lorentz system. *J. Nano-Electron. Phys.* **2018**, *10*, 06019. [[CrossRef](#)]
24. Olemskoi, A.I.; Khomenko, A.V. Synergetic theory for jamming transition in traffic flow. *Phys. Rev. E* **2001**, *63*, 036116. [[CrossRef](#)] [[PubMed](#)]
25. Khomenko, A.V.; Lyashenko, I.A. A stochastic model of stick-slip boundary friction with account for the deformation effect of the shear modulus of the lubricant. *J. Frict. Wear.* **2010**, *31*, 308–316. [[CrossRef](#)]
26. Lyashenko, I.A.; Manko, N.N. Analysis of the stability of stationary boundary friction modes in the framework of a synergetic model. *Ukr. J. Phys.* **2014**, *59*, 87–94. [[CrossRef](#)]
27. Stefanovich, L.; Mazur, O.; Sobolev, V. Formation of regular domain structures in quenched ferroelectrics under the influence of an external high-frequency electric field. *Nanosci. Nanotechnol. Asia* **2019**, *9*, 344–352. [[CrossRef](#)]

**Publisher's Note:** MDPI stays neutral with regard to jurisdictional claims in published maps and institutional affiliations.



© 2020 by the authors. Licensee MDPI, Basel, Switzerland. This article is an open access article distributed under the terms and conditions of the Creative Commons Attribution (CC BY) license (<http://creativecommons.org/licenses/by/4.0/>).